Active Millimeter-wave Imaging for Concealed Weapons Detection*

E. N. Grossman and A. J. Miller
Electromagnetic Technology Division, National Institute of Standards and Technology, Boulder, CO

ABSTRACT

Actively illuminated mm-wave imaging systems for concealed weapons detection offer the possibility of much higher sensitivity than with passive systems. We discuss several issues specific to mm-wave imaging systems that are actively illuminated and describe our implementation of such a system. We show that the illumination geometry is critical to the appearance and detectability of targets, and present measurements of the bi-directional reflectance distribution of a small handgun, as a prototypical target. We demonstrate suppression of standing waves using frequency modulated (FMCW) illumination and directly compare images taken with CW, FMCW, and pulsed illumination. Our implementation of an active imaging system is based on a 120-element focal-plane array (FPA) of uncooled antenna-coupled microbolometers. We describe the fabrication process and yield for these FPA's, as well as tests that show the performance of individual pixels on the 120-element array to be equivalent to that of isolated devices. These results demonstrate that wiring for readout of an antenna-coupled FPA can be made "transparent" to the antennas. Therefore, a mm-wave FPA that is read out through wiring to the perimeter of the array constitutes a simple and feasible architecture, in contrast to the infrared, where space limitations require vertical (3D) integration of readout and FPA. The electrical readout system for the FPA is also described. Finally, we present a result obtained with the full FPA system, showing that 3-way illumination is much more effective for detection of a complex target than a single directional illuminator.

Keywords: Bolometer, array, millimeter-wave, concealed weapons, imaging

1. INTRODUCTION

The high transparency of clothing at millimeter wavelengths and the spatial resolution required to form adequate images combine to make imaging at millimeter wavelengths a natural approach for screening people for concealed weapons, an approach which has been explored by several groups for some time[1,2]. In general, purely passive systems tend to suffer from low sensitivity, making indoor operation problematic, while actively illuminated systems tend to be more limited by glint and other systematic uncertainties in the final images. Although technical means exist to overcome both these issues, the ability to obtain high quality images at adequate speeds, in a system that can be manufactured at low cost has yet to be demonstrated.

In 1999, we began a program to develop active millimeter-wave imagers based on uncooled, antenna-coupled microbolometers (ACMB's) for application to concealed weapons detection (CWD). The first 2-3 years' work focused on design, fabrication, and characterization of single-pixel ACMBs[3,4,5,6]. These earlier papers also describe the overall design of our system, which is based on an operating frequency of 95 GHz. A theoretical sensitivity analysis was also presented. Briefly, the uncooled microbolometers are composed of 20 nm thick Nb, approximately 3 x 10 μm^2 in area, thermally isolated by a thick layer of SiO_2 grown upon the Si substrate. Sensitivity of the microbolometers at frequencies above 1 kHz, where they are operated in our system, is limited by Johnson noise, with an electrical noise-equivalent power of NEP = 50 $pW/Hz^{1/2}$. The microbolometers are coupled to the incident radiation field through a novel modification of an annular slot antenna. The antenna design provides a relatively high directivity (i.e. antenna gain) of 17 dB in a form that is *completely* planar, i.e. there is no substrate lens or micromachined horn integrated with each pixel. This is a critical feature necessary for construction of large, or even moderate-format arrays (e.g. our 120-element design) at reasonable cost. It also provides a highly circular beam, high polarization purity (> 25 dB), the ability to embed two microbolometers for dual-polarization capability, and a circular form factor which eases the wiring/packing problem in an antenna-coupled FPA. The antennas and microbolometers are located on a dielectrically thin Si substrate, (thickness = $\lambda_d/20$ = 50 μm). A reflecting backshort is then placed at $3\lambda_0/4$ behind the antenna plane to reflect the backward lobe of the otherwise symmetric antenna pattern into the forward direction, constructively interfering with the antenna pattern's forward lobe and increasing the directivity. The detailed antenna patterns for this antenna, along with simulations performed with a commercial method-of-moments code, have been presented elsewhere[4]. Overall, the greatest strength of the antenna-coupled microbolometer design is its extreme

Passive Millimeter-Wave Imaging Technology VI and Radar Sensor Technology VII, Roger Appleby, David A. Wikner, Robert Trebits, James L. Kurtz, Editors, Proceedings of SPIE Vol. 5077 (2003) © 2003 SPIE · 0277-786X/03/$15.00

simplicity and robustness, which translate into low cost and ease of manufacturing, while its sensitivity is adequate for the CWD application.

Last year at this conference, we presented the first mm-wave imagery obtained with these microbolometers, obtained by using a single-pixel detector and mechanically scanning the primary collection mirror[7]. The migration path to a 120-element FPA was also presented. In this paper, we present more detailed measurements made with the scanned single-pixel system, which we believe have general implications for active mm-wave imagers. We also describe the implementation and first results obtained with the 120-element FPA. The underlying technical problem addressed by all this imaging work is how best to image highly complex, irregular objects, in arbitrary orientations, with diffraction-limited, or near diffraction-limited spatial resolution.

2. SCANNED SINGLE-PIXEL IMAGERY

The scanned single-pixel system has been described in ref. 7 (see fig. 1 of ref. 7 for a diagram of the optical layout). It consists of the detector assembly, illuminating source, target, and a primary mirror mounted on a stage whose orientation is computer-controlled in both azimuth and elevation. The illuminating source can either be a CW Gunn oscillator or a pulsed Impatt oscillator that emits broadband noise. The system can be configured in two illumination geometries: (a) with illumination from a fixed source flooding the entire target field, or (b) with focused illumination, concentrated at each given moment on the same point of the target to which the detector is sensitive, and which is scanned synchronously with the scanning of the detection beam. (This is accomplished with a segmented focusing mirror, with the inner segment devoted to the illumination beam and the outer to the detector beam.) Although this system is very slow – an image of the field shown in Fig. 1 requires anywhere from .5 to 15 minutes to acquire, depending on sampling – it has been very useful for investigating general features of active mm-wave imaging systems, particularly those related to illumination strategies.

a. Spatial Resolution

A quantitative comparison was made between the measured and theoretical spatial resolutions. The measured value was obtained by calculating the width of the unresolved feature indicated in Fig. 1. The result was 10.4 x 9.3 mm (vertical x horizontal full-width to half-maximum (FWHM)), in an image formed with mirror to target and mirror to detector distances of 1 m each. The theoretical estimate is dominated by simple Airy diffraction from the 30 cm diameter collecting mirror. This yields a 10.5 mm FWHM. However, this width is slightly broadened by convolution with the antenna pattern (which is marginally different in the horizontal and vertical planes), and slightly narrowed because of the scanned illumination, yielding an overall theoretical width of 9.9 mm FWHM, in excellent agreement with measurement. In this configuration, the single-pixel system is clearly diffraction-limited.

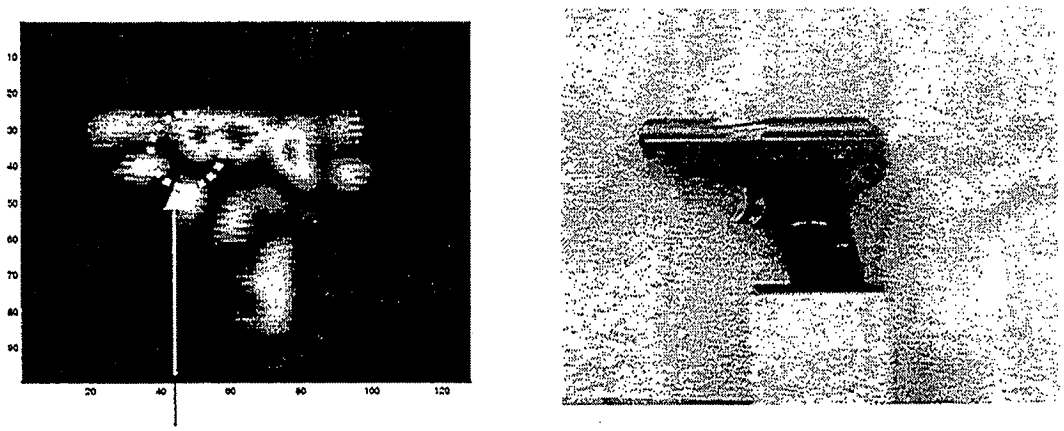

Fig. 1. Mm-wave image and optical photograph of a small handgun obtained using the scanned single-pixel system. The unresolved feature used to evaluate system spatial resolution is indicated. This image was deliberately oversampled by a factor of 4 to avoid any influence of sampling issues on the evaluation of spatial resolution.

b. Illumination Mode

It has often been asserted that one of the chief drawbacks of an active system is glint in the images arising from uncontrolled standing waves between the target and its environment. This only applies to illumination by coherent sources with a fractional bandwidth less than the fractional differences in path length. The broadband noise source (fractional bandwidth 5 %) does not have this. In order to assess the importance of the standing wave issue, we performed a direct side-by-side comparison of illumination with CW, frequency-modulated CW (FMCW), and pulsed broadband radiation, as shown in Fig. 2. Frequency modulating a CW source varies the period of any standing waves. When the frequency of modulation is faster than the detection time constant, and the amplitude is sufficient to sweep the standing wave pattern through at least one full period, all effects of the standing waves will be suppressed. In the measurements we performed, the CW and FMCW sources were amplitude modulated at a low frequency, typically 100 Hz, and the bolometer signal synchronously ("lock-in") detected with a time constant of 30 ms. This time constant sets the speed of frequency modulation in the FMCW measurements. The modulation frequency was typically 10-100 kHz, and the modulation amplitude approximately 400 MHz. The first panel directly demonstrates the resulting suppression of standing waves, generated in this case by moving the target along the direction of the beam and monitoring the signal from a single pixel.

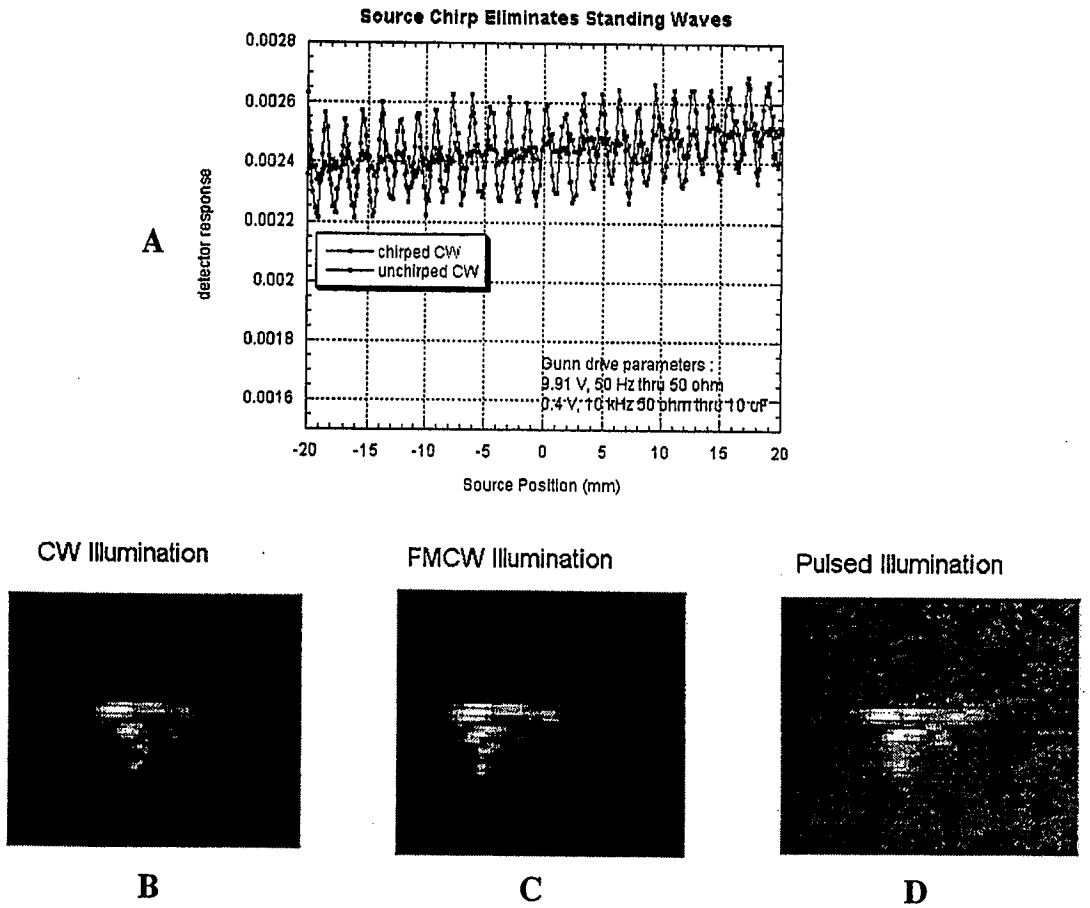

Fig. 2. The upper panel (A) illustrates the suppression of standing waves obtained by frequency modulating ("chirping") the CW Gunn oscillator. Panels B-D illustrate handgun images taken with different mm-wave illumination sources, a CW Gunn oscillator(B), frequency modulated CW Gunn oscillator (C), and a pulsed, broadband noise source (D), all three operating at 95 GHz.

Three images, obtained with the scanned single-pixel system, using CW, FMCW, and pulsed broadband noise illumination, are shown in Fig. 2. They are most remarkable for their overall similarity. The pattern of hotspots and deep minima running through the image, which is rather flat in an optical photograph, is nearly identical in the three cases, indicating that it is not

caused by standing wave structure. An additional conclusion can be drawn from the images shown in Fig. 2. The power available from the Gunn oscillator used for the CW and FMCW images was ~ 40 mW, while the average power available from the pulsed broadband noise source was approximately 4.5 mW. The quality of the image taken with the pulsed broadband source is however, comparable to or slightly better than the other two. Although the comparison is not quantitative, it lends support to the original sensitivity analysis, which indicated an advantage in sensitivity for an architecture based on pulsed illumination and gated integration This sensativity scales with the square root of duty cycle and linearly with average power. For our particular sources, the advantage of the pulsed architecture is almost completely counterbalanced by the lower average power of the pulsed source.

c. Hotspots and Deadspots

The structure visible in the handgun images -- bright spots separated by deep minima, without any counterparts in an optical photograph, , demands some explanation, given that it is not related to standing-wave effects. Two initial observations led us to suspect this hotspot structure was related to illumination geometry. First, obtaining easily recognizable images of the handgun like that in Fig. 1 required some alignment of the target's orientation. Second, scans of reflected signal (on a single pixel) as the target was rotated, as shown in Fig. 3, were very complex - much more complex than the simple assumption made in our original sensitivity analysis, of 50 % total diffuse reflectance isotropically distributed over 2π srad. Indeed, we followed this with a series of full images taken with varying target orientations, and fixed illumination and detection angles. Most of these images show signal from only one or another part of the handgun, typically an edge. In many cases, the bright edge corresponds to a bright edge in the corresponding optical photograph. The latter, in turn, is clearly due to specular reflection of the flash illumination used to take the optical photograph. Moreover, the mm-wave image is much brighter and covers the full area of the handgun when the handgun is oriented broadside, so as to specularly reflect the illumination beam back into the collecting aperture. Although by animating the images into a synthetic "movie," it is possible to recognize the rotating handgun at other orientations than broadside, the off-broadside images are individually not very recognizable. More importantly for CWD applications, there existed particular target orientations in this experiment for which no signal was observable above the noise floor – that is, there were dead spots in the image due to target orientation. We have concluded from this, and from comparison with the optical images taken with the same system geometry, that the complex "hotspot" structure is caused by strong specular reflections or "glint" off the particular regions of the target whose surface is oriented properly, and into the collecting aperture. (This is analogous to the glint sometimes seen in indoor optical photographs taken with a flashbulb.) The conclusion is that active mm-wave imaging systems must use a more sophisticated illumination system, with radiation incident from multiple directions (ideally a diffuse illuminator), and must have sufficient sensitivity to image diffuse, non-specular reflection from the target.

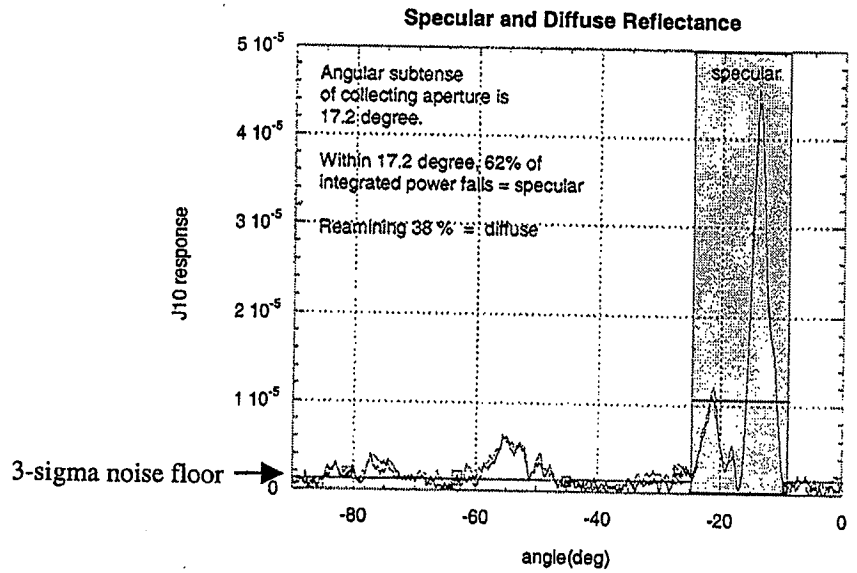

Fig. 3. Reflected signal from the handgun onto a single pixel, as the handgun is rotated in azimuth. This is equivalent to a plot of bidirectional reflectance distribution (BRDF) from a representative point on the handgun surface. Areas where the reflected signal falls below the noise floor are "deadspots".

3. FOCAL PLANE ARRAY RESULTS

Concurrently with imaging using the scanned single-pixel system, we have built the originally planned, full FPA-based system to enable much faster imaging than is possible with the scanned single-pixel system. Our FPA design consists of a 120-element array, covering a full 75 mm diameter wafer. Wiring for each pixel is brought out to the perimeter of the wafer in four quadrants; within each quadrant, the wiring is oriented nearly perpendicular (82°) to the polarization of all the pixels in that quadrant, given by the E-plane of that quadrant's antennas. The perpendicular orientation of the wiring to the antennas' E-plane is intended to make the wiring "transparent" to the antennas. Otherwise, the antenna properties would be highly perturbed by electromagnetic coupling to the wiring. The array pitch is 4.75 mm, approximately 1.5 free-space wavelengths. This was selected on the basis of two observations.[4] First, the unusually narrow antenna pattern measured on single-pixel devices implies a directivity of 17 dB, which corresponds, via the antenna theorem, to an effective area of approximately 6 x 6 mm. Secondly, a direct measurement was made of the beam pattern of an isolated antenna, an antenna at the center of a 5-element array on 2.5 mm pitch, and an antenna at the center of a 5-element array on 5 mm pitch. At the 5 mm spacing the pattern was identical to the isolated device, but at 2.5 mm spacing there was a substantial broadening of the pattern with higher sidelobes and asymmetry. The 4.75 mm spacing was judges to be sufficiently distant to preserve the isolated device performance.

a. Fabrication, pixel performance

The chief challenge in fabricating the 120-element FPA was that of fabrication on the 50 μm thick substrate. Initially, this was done by fabricating the FPAs on pre-thinned, 50 μm thick wafers, laminated to thick backing wafers, and then de-laminating the FPA at the end of the fabrication process. FPA's were successfully fabricated by this technique, and we verified that the performance of FPA pixels matched that of the single pixels tested earlier in the program. This test consisted of comparing the optical response of a single-chip, isolated microbolometer with that of a single pixel from the center of the 120-element array, as a focused mm-wave beam was scanned across the pixel. Both the amplitude and shape of this response were very similar for the two cases. This demonstrated that the strategy of running readout wires to the perimeter of the array, perpendicular to the antenna polarization, is indeed a feasible one for antenna-coupled arrays. It is a significant point because of the simplicity of this approach, and the ability it provides to decouple the readout system from the FPA. It is important to realize that this approach is impossible in infrared FPA's, because the much smaller pixel spacing, typically 50 μm, does not allow enough space for running wires to the array perimeter. Therefore, vertical (3D) integration of FPA and readout is required in the IR. While elegant solutions to enable this have been developed[8], their use is unnecessary at mm-wavelengths.

The FPA fabrication process based on lamination of pre-thinned wafers was not as robust as hoped; the 50 μm thick wafers were fragile and yield was low. We therefore migrated to a process based on deep reactive-ion etching (DRIE) to thin the substrate from the back after the FPA has been produced. At the same time, other improvements were made to the FPA design: in particular, the Nb bolometers were passivated with an overlying layer of SiO_2 to improve their lifetime (it also allows them to be run hotter, and therefore with higher sensitivity) and the wiring crossovers necessary for the design were integrated into the lithographic process, eliminating the previous need for complex manual wirebonding. Fig. 4 displays a completed FPA wafer built with the new process. The fabrication is now a 5-level process, compared to the earlier 2-level one, but the improvement in reliability (both FPA strength and bolometer lifetime) renders it worthwhile.

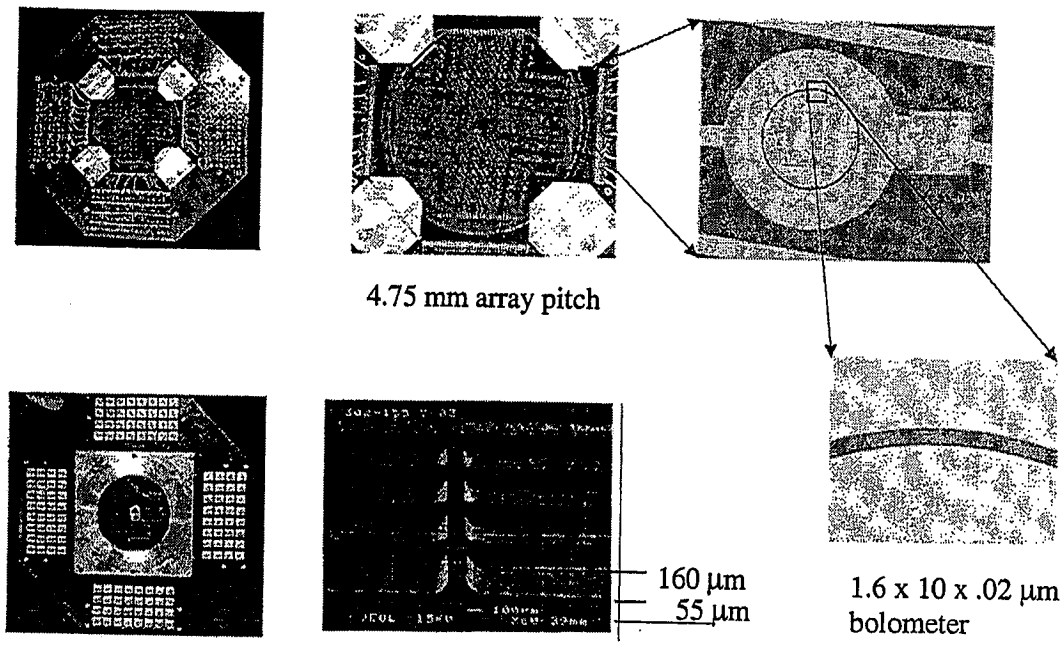

Fig. 4. Several views of the completed 120-element FPA. The lower left and lower middle panels display the back side of the FPA, with the adjustable backshort removed.

b. Readout system

As described in previous papers[7], the FPA-based system uses for illumination high power Si IMPATT (impact ionization avalanche transit-time) oscillators, operating at 95 (± 2.5) GHz in pulsed mode. Their peak power is 0.45 W, delivered in 100 ns pulses at a 100 kHz repetition rate. They are commercially available, at low enough cost to avoid prohibitive impact on overall cost for a practical system. The readout of the array is a "brute-force" repetition of 120 channels of preamplification and gated integration. A block diagram of the overall system is shown in Fig. 5. Each microbolometer is current biased, ordinarily at ~ 5 mA, and presents a 150 Ω source. The front-end preampifier must be very low noise to avoid adding to the fundamental Johnson noise of the microbolometer; this system provides noise performance of approximately 0.9 $nV/Hz^{1/2}$, with a 5 MHz bandwidth. Each microbolometer's output feeds a separate channel of fast analog pre-amplification and gated integration, located off-wafer. The gated integration is accomplished by converting each amplified output to a current (via a resistor), and then switching the current onto an integration capacitor during the gate window. A commercial computer-controlled timing generator controls the gating of the integrator as well as the pulsing of the sources and the triggering of the data acquisition system.

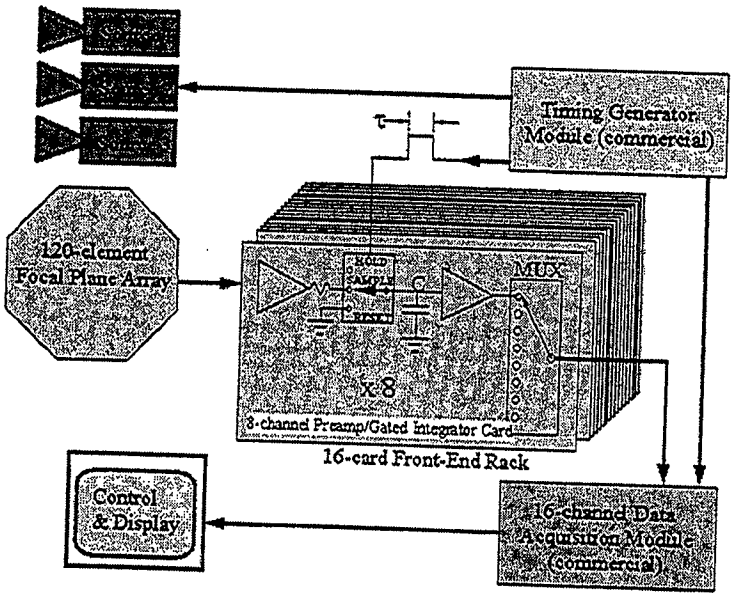

Fig. 5. Block diagram of the of the FPA-based imaging system, (omitting optics), indicating preamp/gated integration modules.

The throughput of the system is a significant design challenge. With three sources each running at 100 kHz, the analog multiplexer (MUX) runs at 2.4 MHz, and the 4 data acquisition modules, which each read out a quarter of the array, each digitize at nearly 10 MS/s. The integration of many samples (typically ~2000-3000) to reduce the throughput to a 30 Hz frame rate is done in the host computer. The total data rate into the computer is ~ 80 MB/s, which noticeably loads the PCI bus. In a more practical system, the integration of the samples could be done with a dedicated ASIC.

c. 3-way illumination system

Both as an initial test of the complete FPA-based system, and as a means of addressing the issues associated with a single directional illuminator, a system was assembled which incorporated 3 separate, pulsed broadband illuminators. The system is illustrated in Fig. 6. The sources illuminate the target from 3 mutually orthogonal directions, while the target is viewed from a direction lying within the octant defined by the three illumination beams. Each source is projected through a pyramidal, 24 dB standard-gain horn, which provides a ~20 cm wide beam at the target. The collecting aperture is the same 1 m radius of curvature spherical mirror used in the scanned single-pixel measurements. The distance from target to aperture and FPA to aperture are both 1 m, resulting in a magnification of 1:1. The three sources are triggered sequentially, each at 100 kHz, while the integrator is gated at 300 kHz. Because the signal from every pixel is digitized and recorded during every gate period, the signals from the individual illuminators can be separated out, and displayed in real time as three separate colors on the monitor, or they can be summed and displayed as a grayscale image.

Fig. 7 displays the signal obtained from the entire array, as the handgun is rotated in azimuth. It is thus a BRDF-type plot analogous to Fig. 3, but with the critical difference of including multiple illumination sources. The specular reflectance off the broadside faces of the target, from the two illuminators lying in the plane of rotation, are obvious. The key result however, is that, although there are target orientations at which the signal from one individual source falls below the noise floor, there are no deadspots. At every orientation there is easily detectable signal from at least one, and usually two of the illuminators. If this conclusion is true in general for all complex targets, it is an extremely significant and encouraging result for the use of mm-wave imaging for CWD, since it implies that threat items can always be detected, regardless of orientation.

Finally, the spatial resolution of the FPA-based system was evaluated by removing the target and putting in its place one of the pulsed noise sources, with its feedhorn removed. The open-ended W-band waveguide provides a good approximation to a point source in the object plane of the system. The resulting FPA readout is shown in Fig. 8. Clearly the level of crosstalk is minor, indicating the system is reasonably well in focus and aberrations are low.

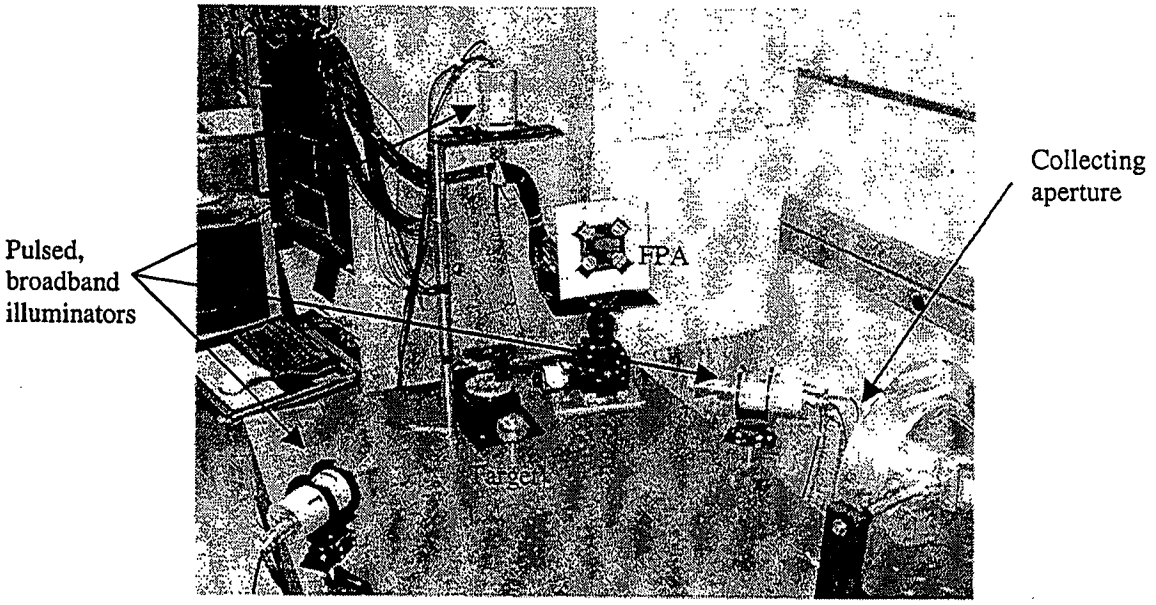

Fig. 6. 3-way illuminated, FPA-based imaging system

4. CONCLUSIONS

Using a mechanically scanned single-pixel mm-wave imaging system, we have obtained imagery of a handgun, a complex metallic target typical of threat items likely to be encountered in CWD applications. Images taken with CW, FMCW, and pulsed broadband noise illumination were directly compared and found to be very similar, indicating that standing waves have little effect on such imagery. Spatial resolution is well predicted by simple diffraction. However, when a single directional illuminator is used, the images are dominated by spurious hotspots created by specular reflections off particular areas of the complex target geometry. "Dead" orientations of the target, where no detectable signal is seen, are also found. With illumination from multiple directions however, no dead orientations are observed. The latter observation was made using a 120-element FPA equipped with real-time readout.

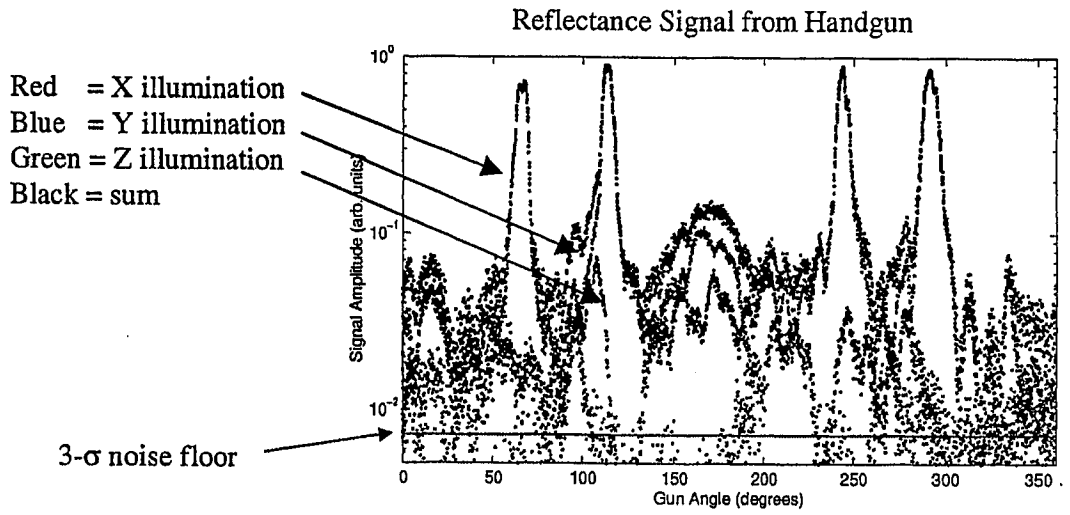

Fig. 7. Reflected signal from the handgun onto a the entire array as the handgun is rotated in azimuth. Note the absence of "deadspots" (cf. Fig. 3)

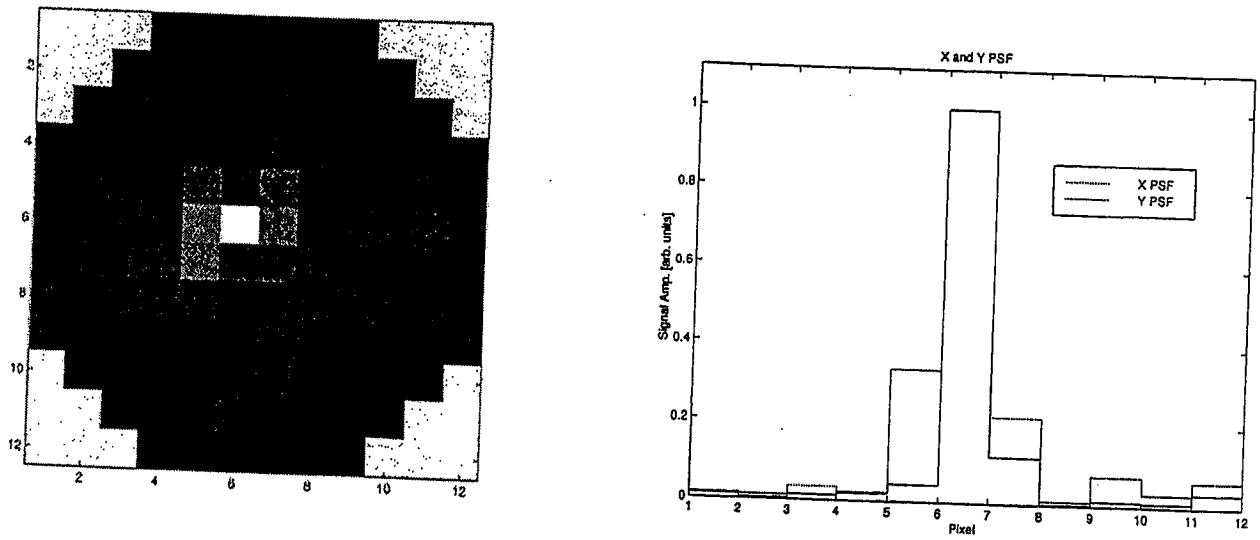

Fig. 8. FPA image of a point source, as described in the text.

5. ACKNOWLEDGEMENTS

We are grateful to Nick Paulter of NIST, Gaithersburg for initiating this project and providing extensive advice on requirements for the end use. We are also grateful to Steve Waltman quickly debugging the electronics for the 120-channel readout system under considerable time pressure, to A.K. Bhupathiraju for assistance with FPA fabrication, and to Norm Bergren for technical support. We thank the National Institute of Justice and the Federal Aviation Adminisitration, which provided financial support for this program, through the NIST Office of Law Enforcement Standards.

6. REFERENCES

[1] P.F. Goldsmith, C.-T. Hsieh, G.R. Huguenin, J. Kapitzky, and E.L. Moore, "Focal Plane Imaging Systems for Millimeter Wavelengths", *IEEE Trans. Microwave theory and Techniques*, **41(10),** pp.1664-1675 (1993)

[2] A. R. Luukanen, V.-P. Viitanen, "Terahertz Imaging System based on Antenna-coupled Microbolometers", *Proc. SPIE,* **3378,** pp. 34-44 (1998)

[3] S. Nolen, J. A. Koch, N. G. Paulter, C. D. Reintsema, and E. N. Grossman, "Antenna-coupled Niobium Microbolometers for Millimeter-wave Imaging Arrays",*Proc. SPIE* **3795,** pp. 279-286, (1999)

[4] S. Nolen, T. E. Harvey, C. D. Reintsema, and E. N. Grossman, "Slot-ring Antennas with a Planar backshort Designed for Millimeter-Wave Applications",*Proc. SPIE* **4373,** pp. 49-57 , (2001).

[5] E. N. Grossman, S. Nolen, N. G. Paulter, C. D. Reintsema, " Concealed Weapons Detection System using Uncooled, Pulsed, Imaging Arrays of Millimeter-wave Bolometers", *Proc. SPIE* **4373** pp. 7-15 (2001)

[6] . G. Paulter, E. N. Grossman, G. N. Stenbaken, B. C. Waltrip, S. Nolen, and C. D. Reintsema, "Design of an Active Mm-wave Concealed Object Imaging System",*Proc. SPIE* **4373,** pp. 64-71, (2001).

[7] E.N. Grossman, A.K. Bhupathiraju, A.J. Miller, C.D. Reintsema, "Concealed Weapons Detection using an Uncooled Millimeter-wave Microbolometer System", *Proc. SPIE,* **4719,** pp.364-369 (2002)

[8] R. A. Wood, "Monolithic Silicon Microbolometer Arrays", chap. 3 in *Uncooled Infrared Imaging Arrays and Systems,*P.W. Kruse and D.D. Skatrud eds., Academic Press, San Diego, (1997)